Hindawi
Journal of Electrical and Computer Engineering
Volume 2022, Article ID 7001448, 12 pages
https://doi.org/10.1155/2022/7001448

Research Article

Designing of Neuro-Fuzzy Controllers for Brushless DC Motor Drives Operating with Multiswitch Three-Phase Topology

Ch. Vinay Kumar,[1] G. Madhusudhana Rao,[2] A. Raghu Ram,[3] and Y. Prasanna Kumar[4]

[1]*MGIT, Hyderabad, India*
[2]*OP Jindal Univesity, Raigarh, India*
[3]*JNTUCEH, Hyderabad, India*
[4]*Bule Hora University, Oromia, Ethiopia*

Correspondence should be addressed to G. Madhusudhana Rao; gmrgurrala@gmail.com and Y. Prasanna Kumar; prasannaky@gmail.com

Received 2 May 2022; Revised 24 May 2022; Accepted 30 May 2022; Published 20 July 2022

Academic Editor: Ton D. Do

Brushless DC motors are simple in construction, high efficiency, less noise, and high reliability, which are not replaceable motors in specific applications compared to other motor drives. It has a facility for its multivariable system, nonlinear control process, and powerful coupling system. This paper proposes to design the neuro-fuzzy controllers for its multiple converters switching to improve the power factor and minimize the BLDC motor switching losses. Compared with conventional controllers, this controller will develop the power factor and optimize the current ripples concerning time and torque. The working model of the BLDC motor may be presented here. A nonlinear load will be applied to the BLDC motor to determine the speed, current, and torque. The multiple switches designed with the proposed controllers are connected with the converter's DC link to boost the voltage. The fuzzy logic controller is implanted to adjust the speed of the neural network and is also designed for the analysis of the stability of the system. The proposed controllers compare the rate at different speeds, torque, currents, and rotor angle positions. Finally, the proposed controller for multiple converter switches performs better than the conventional controllers.

1. Introduction

In recent years, brushless DC motors have become more popular and valuable in industries due to their highly reliable power density and ease of handling. The converter circuit will be used to control the brushless DC motor in three-phase systems. The rotor position sensor will be used for the start and a suitable communication pattern to operate the bridge circuit so that the power devices are commutated for every 60°. To meet the requirement of the efficiency and performance of the BLDC motor requires properly suitable speed controllers. In conventional motors, speed control is achieved by the PI controllers due to their simple construction and implementation in an industrial application. But when the motor is connected to a nonlinear type of load, the motor parameters are altered, the disturbances will occur that cannot easily control the speed of the motor.

Furthermore, the conventional controllers need exact mathematical models to find the speed response and steady-state error, and power factor enhancement of the BLDC motor, which is not for many sufficient controllers. Due to overcoming these disadvantages of the PI controllers, artificial intelligence controllers like fuzzy logic, neural network, and adaptive neuro-fuzzy controllers may be implemented to control the speed of the BLDC motor effectively. The converter is used with the five-level switches in this proposed paper. In maintaining the speed of the BLDC motor, it is necessary to design the ANFIS controllers to achieve the best performance and efficiency [1]. Different computing

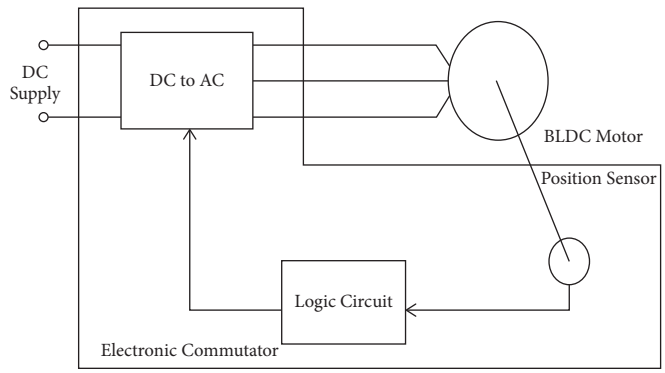

Figure 1: Constructional features of the BLDCM.

methods are available to approach the requirement to solve the current difficulties in controlling the speed of brushless DC motors. In this paper, a new novel soft computing method is applied to overcome the problems like current distortions and voltage issues of the brushless DC motor using the neuro-fuzzy logic controllers to compare the PID controllers. In neural networks, the inputs are well trained and tested, showing the helpfulness of the controller and governing the speed and steady-state errors, etc. Tuning the PID controllers with the proposed controllers has improved performance and caused higher efficiency than the PID controllers [1]. The three-phase converter circuit will be used to control the brushless DC motor. It needs the rotor position sensor for the controlling process of the converter to obtain suitable swathing conditions, which will minimize the switching losses.

In general, the Hall sensors will be used to evaluate the revolving position of the rotor by specific parameters applied to the positioning of the sensor using well-developed sensor technologies [2, 3]. These sensor positions are electrically driven every phase by 1200, divided into 60° for every step. One instant at a time, only two phases will be carried out. This phenomenon will be shown in Figure 1. From Figure 1, we can understand the brushless DC motor model and its performance with the elements of the motor. The simulation of the equivalent and operational circuit of the brushless DC Motor is shown in Figure 2. The speed sensor is coupled with the brushless DC motor with the three-phase converter to maintain the current, providing the BLDC motor to adjust the current. This sensor produces the control signal to evaluate the PWM, which activates the converter drivers. The Hall sensors will be working to converter circuit drive for the essential switching stage. These crucial stages of the switches will allow the normal condition of the three-phase converter to prevent the short circuit in any of the three legs or three lines. The brushless DC motor flux distribution and EMF waveforms are generally similar to the trapezoidal one. When the BLDC motor is operated in self-controlled mode, the EMF waveforms are similarly sinusoidal, so the BLDC motor is called the sinusoidal BLDC motor.

So the sinusoidal BLDC motor and trapezoidal BLDC motor are very similar. In these two cases, the rotor position must be synchronized then the motor currents may be controlled. Though there are constructional differences

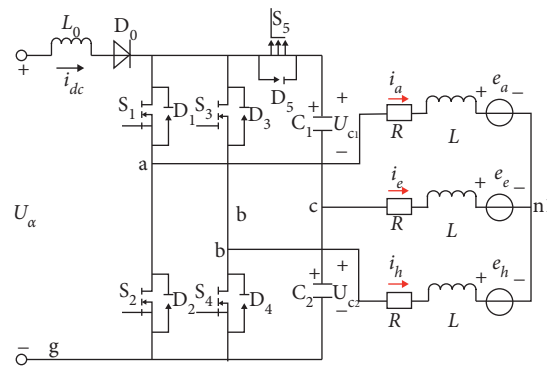

Figure 2: Equivalent and operational circuit of the BLDC motor.

between the synchronous motor and trapezoidal BLDC motor, the excitation of the current is different in both machines. The BLDC motor's current is excited by the square wave or quasi-wave currents. The Hall sensor devices detect the rotor EMF and evaluate the phase switching points of the trapezoidal BLDC motor. The sinusoidal BLDC machine needs the sequence of the exact position of the rotor, and then it will allow the correct combination of the sinusoidal waveforms. Therefore, the BLDC motor has a significant role in designing factors over the standard DC motor. The shaft position of the sensor system is modest and essential only to allocate the number of signals for imposing the transistor of the converter. The quasi-square armature currents will directly control machine torque by their maximum amplitude value. The natural dead time for every transistor is most reliable to improve the performance of the converter in the BLDC motor. The synchronization process is allowed to operate the machine, and it required the first and third characteristics which will minimize the complexity in the circuit of the machine circuit [4], but the second characteristics will allow the circuit which will design for the DC machine for controlling the trapezoidal current $I_{\max}$.

This proposed paper uses the neuro-fuzzy controllers for this BLDC motor to control its speed and minimize the current distortions. The fuzzy logic will be used for time optimization, and the neural network will be implemented to test and train the parameters. These two controllers are integrated and give the perfect result of the BLDC motor. The implementations of the fuzzy controllers will work

based on the rule base function with the IF-THEN rule, where it is easily understandable for the drive. In neural networks, the supervisory learning method will be used to overcome the drawbacks of backpropagation. This proposed controller is used for the estimation of the torque and speed of the BLDC motor drive. The operational capability of the deliberated controller is explained in detail in MATLAB/Simulink simulation results [5].

2. Modelling of the BLDC Motor

In the BLDC machine, the stator winding is concentrated. Hence, the stator waveform will be trapezoidal, whereas in PMSM, the stator winding is distributed winding. Hence, the stator waveform is sinusoidal. As far as the rotor is concerned, both are permanent magnets. It is also comparable to constructing an AC motor with the BLDC motor. The constructional features of the brushless DC motor are shown in Figure 1. Majorly, the stator windings are similar to the three-phase induction motor, and several permanent magnets are placed in the rotor. The main dissimilarity between the AC motor and the BLDC motor is that the location of the rotor of the BLDC motor produces the signal to control the switching operation of the switches. The Hall sensor is the main common element in the DC motors, but some other special DC motors use optical sensors [6].

According to the six states, the brushless DC motor will work according to the working principle. Two phases will be active in each state as per the operating principle. The generalized conceptual waveforms of the back EMF of the BLDCM are characterized in Figure 3 [3]. The developed model of the brushless DC motor comprises the back EMF and phase inductance of the rotor. e_{MAX} is the maximum error that will be evaluated based on the inclines of m_1 and m_2 at the functioning of the carrier frequency. This phenomenon is described in the following mathematical equations:

$$|m_1| = \frac{E_{pp}}{xT} = \frac{E_{pp} \cdot f}{X}, \tag{1}$$

$$|m_2| = \frac{E_{pp}}{(1-x)T} = \frac{E_{pp} \cdot f}{1-X}, \tag{2}$$

where

$$x = \frac{|m_2|}{|m_1| + |m_2|}, \tag{3}$$

$$E_{pp} = \frac{1}{f}\left(\frac{|m_1| * |m_2|}{|m_1| + |m_2|}\right). \tag{4}$$

In the case of incremental in current, the term "x" in the above equation (3) denotes the carrier "T" period. From equation (4), "x" describes a model production of the pulse width modulation design. So the regulating constraints must be familiar with "x." Finally, E_{PP} characterizes the maximum error signal.

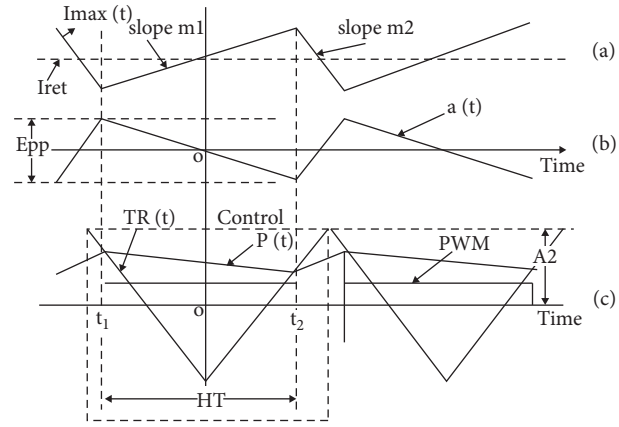

Figure 3: Generalized graphical representation of (a) feedback signal I_{MAX}, (b) error signal $e(t)$, and (c) control signals [D_1] [7].

The constructional features of the three-phase BLDC motor are as shown in Figure 3, similar to the permanent magnet synchronous motor [7]. In this construction of the BLDC motor, it is observed that the stator windings are the same as the AC motor, and the rotor is designed with permanent magnets. But the BLDC motor differs in rotor position to generate the control signal in electronic circuit switches. The Hall sensor is used to control the rotor position by using switches. The BLDC motor will be working with the six-state principle, and each state will be working with the concept of the two-phase principle [3]. Figure 3 clarifies the commutation process in the BLDC motor according to the working idea of the rotor position.

Figure 2 shows that the brushless DC motor uses the direction of the Hall sensor to make the commutation process per the rotor position. The MOSFET is designed in the converter circuit. It will conduct the conduction process and generate the EMF in three phases A, B, and C of the brushless DC motor. The commutation process will follow as per the rotor position. The three-phase currents will be commutated at every 60° electrically in BLDC motors. These commutating signals will be identified and received by the hall sensors of the rotor system. However, the signals will be divided into six modes of operation as per the switching pattern in the converter circuit, and each of the two switches will act at one time in a two-phase system, and the other one is off-mode. From Figure 2, it is analyzed that the proposed algorithm and conventional topology designed the BLDC motor drive system is presented here. The figure consists of three-phase currents i_a, i_b, i_c; back EMF of each phase e_a, e_b, e_c; resistance R (r_a, r_b, r_c), inductance L (L_a, L_b, L_c) of each phase, i_{dc} is the DC-link current, "n" is the ground point to the winding of the stator of the designed BLDC motor drive system. The DC-link is a capacitor directly connected with the ground terminal from phase C. The red-coloured arrow marks show the direction of the three-phase currents. Using the neuro-fuzzy controllers, the voltage must be enhanced between the capacitors C_1 and C_2 with the proposed new technology. It causes the consumption of the supply voltage, which must be increased in case of the low supply voltage. The inductance L_0 will store the energy and boost when the

drive system's vector system is working. The switches will be turned-on alternatively with a continuous process of the proposed topology. During this process, the storage of energy by the inductance L_0 will be given to the capacitors to increase the voltage when the switches are in the turn-off position. But the diode D_0 will block the reverse energy, then it may flow DC-link to the power supply to switch on the other switch 1. In this way, the designed BLDC motor drive system will work with the proposed new technology.

The typical mathematical equations of the BLDC motor are described due to their similarity in its phases, that is,

$$r_a = r_b = r_c = r_m, L_a = L_b = L_c = L_m. \tag{5}$$

The BLDCM designed in the following equations:

$$\begin{bmatrix} u_a \\ u_b \\ u_c \end{bmatrix} = \begin{bmatrix} \mathbf{R} & 0 & 0 \\ 0 & R & 0 \\ 0 & 0 & R \end{bmatrix} \mathbf{X} \begin{bmatrix} i_a \\ i_b \\ i_c \end{bmatrix} + \begin{bmatrix} L_m - M & 0 & 0 \\ 0 & L_m - M & 0 \\ 0 & 0 & L_m - M \end{bmatrix} \frac{d}{dt} \begin{bmatrix} i_a \\ i_b \\ i_c \end{bmatrix} + \begin{bmatrix} e_a \\ e_b \\ e_c \end{bmatrix}. \tag{6}$$

The above equation states that r_m, L_m, and M are the stator resistance, inductance, and mutual inductances, and u_x, e_x, and i_x, are the phase voltage, back EMF, and phase current of the stator [8]. Finally, the EMF torque is expressed as

$$T_e = \frac{Z_P}{2\omega_e} \left(e_a i_a + e_b i_b + e_c i_c\right). \tag{7}$$

From the above equation, ω is the speed of the rotor, and Z_p is the rotor's magnetic poles [9]. Therefore, the motor motion equation can be written as

$$T_e = T_L + J\frac{d\omega_r}{dt} + B\omega_r. \tag{8}$$

3. Neuro-Fuzzy Control Systems

There is a considerable development in the control systems by implementing artificial controllers to control the speed of the machines, which are majorly used like fuzzy logic controllers, neural network controllers, genetic algorithms, and expert systems. These controllers have a particular type of superiorities.

In designing the neuro-fuzzy controllers, the suitable controller is identified from the following explanation; the controller represents the rules at the first level of the approach. The controller's input is quantitative variables, giving the output in linguistic qualitative manner. Then it provides a detailed analysis of the plant and approximates its knowledge. This will work mainly in the following aspect [10]:

(i) Knowledge demonstration and inference are moderately straightforward.

(ii) Rugged construction and operation.

The fuzzy logic controller is the crispy set invented by Lofty Zadeth in 1965. The crisp set is also called the universal set. Takagi and Sugeno proposed the modified fuzzy membership function based on IF-THEN rules which can be applied to the linear equations. The fuzzy logic membership functions are shown in Figure 4, and the error analysis of the fuzzy logic controller is shown in Figure 5.

The fuzzy output model expression will be written as

$$\begin{aligned} Y &= \frac{\sum_{i=1}^{N} w_i y_i}{\sum_{i=1}^{N} w_i} \\ &= \frac{\sum_{i=1}^{N} w\left(C_{i1} + C_{i1}T_1 + \ldots + C_{i1}T_n\right)}{\sum_{i=1}^{N} w_i} \\ &= \frac{\sum_{i=1}^{N} w_i y_i \sum_{i=1}^{N} wC_{ik}T_k}{\sum_{i=1}^{N} w_i}, \end{aligned} \tag{9}$$

where $x_0 = 1$, ω_i is the weight of the i^{th} IF-THEN rule for the input and is calculated as

$$w_i = \prod_{k1}^{n} A_{ik}(xk), \tag{10}$$

where $A_{ik}(x_k)$ is the membership grade.

The fuzzy logic control method can be implemented in ambiguity or uncertainty systems. In the control process of the control system, the membership functions used are generally 10 and 1 in nonlinearity, load distortions, and parameter variation [7]. The neural network evaluation and data treating method simulate the procedure that starts in biological neurons. A neuron is a fundamental element, and the connection of two neurons may work like turned on, trained off, and combining both conditions.

The fuzzy logic controller is designed with the rule-based system. The original concept of the fuzzy logic systems is that they will provide the knowledge representation about the constant parameters. Figure 6 analyses the significant parts of the fuzzy logic [11, 12].

The following rule base is given for a modified T-S fuzzy model

$$\begin{aligned} &If\ X_1\ is\ A_{i1}, \ldots, X_n\ is\ A_{in}\ then\ y_i \\ &\quad = K_i\left(c_0 + c_1 x_1 + \ldots + c_{nx_n}\right), \end{aligned} \tag{11}$$

where $i = 1, 2, 3, \ldots, X_n$ and n are the numbers of IF-THEN rubrics. Therefore, the free parameters will be optimized to the next level. This simplified T-S fuzzy high predictive property model has effectively identified the nonlinear control systems [13]. Using the fuzzy rule foundation must be effectively embedded into the systems that deal with the issues. Progress has been made to systematically improve the fuzzy systems with the creative process [14]. The need to successfully modify the parameters and construct fuzzy

e/ce	NB	NM	NS	ZO	PS	PS	PB
NB	NB	NB	NB	NB	NM	NS	ZO
NM	NB	NB	NB	NM	NS	ZO	PS
NS	NB	NB	NM	NS	ZO	PS	PM
ZO	NB	NM	NS	ZO	PS	PM	PB
PS	NM	NS	ZO	PS	PM	PB	PB
PM	NS	ZO	PS	PM	PB	PB	PB
PB	ZO	PS	PM	PB	PB	PB	PB

Figure 4: Fuzzy logic membership functions.

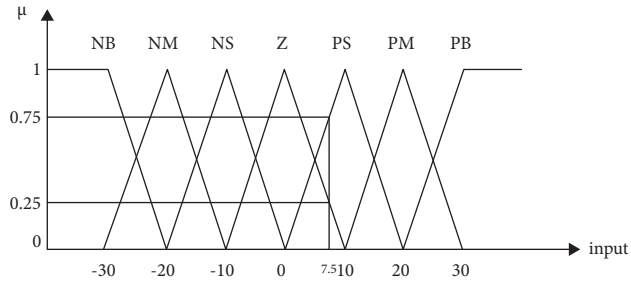

Figure 5: Fuzzy logic analysis of the error.

systems has caused these studies' growth. Many researchers use genetic algorithms, evolutionary programming, and other possible methods to identify the fuzzy logic to design the control parameters. However, the problem of dynamically separating the input space for each input and output variable, selecting the suitable fuzzy rules [15] for which resembling nonlinear systems are unknown, and atomizing the discrimination remains. T-S fuzzy modelling has been designed and developed to model the BLDCM. The speed error and current error of the motor are given to the fuzzy systems as inputs. The speed error can be determined by considering the armature current and the previous error of the armature current I_a. These two errors are fed to the fuzzy controller as per its designed sequence and converted into the linguistic set. Then the defuzzification process will be done. The error and change in "error" of functions are analyzed.

3.1. Pattern and Batch Training. To analyze the pattern mode example, get trained and then the weights are almost updated. Once each training sample is updated, the weights are updated in the epoch mode. The batch mode examples follow the error function's original vertical level, give an idea about it, and discover a set of weights corresponding to the minimum error functions. A sigmoid is used rather than a rugged preventive linear threshold unit. The sigmoid is differentiable, and there is a dissimilarity between an LTU and a sigmoid. The algorithm's calculations are accepted as single layer at one time in parallel. The following is the primary strategy for using the backpropagation algorithm: the desired activation will be [1, −1] rather than the standard [0, 1]. There is both theoretical and experimental evidence. The step size, p, is set to a little positive value. Even while a higher p number leads to faster convergence, this is only true up to a point. When the value of p is too large, the algorithm becomes unstable and fails to converge. As a result, this will be suggested that the rate of p should be kept high determined to 0.1. The starting optimized weights will be distributed casually. The consequences should be observed for a cell with z inputs between $[-2/z, 2/z]$.

(i) Forward propagation computes every cell's weighted sum, Si, and stimulation, $u_i = f(Si)$.

(ii) Backpropagation is completed from the output, and layers are one by one in form. The error correction rules adjust the synaptic weights in this development. From the above equation, the weights are updated

$$W_{ij}^{*} = W_{ij} + p\delta u_j, \tag{12}$$

AMS (approx mean square) error [16]

$$W_{ij}^{m}(\mathrm{k}+1) = W_{ij}^{m}(k+1) - \alpha \frac{\partial \widehat{f}}{\partial w_{ij}^{m}},$$
$$b_{j}^{m}(\mathrm{k}+1) = b_{i}^{m}(k) - \alpha \frac{\partial \widehat{f}}{\partial w_{i}^{m}}. \tag{13}$$

The biological neuron is the foundation of artificial neural networks science. The neuron's essential parts must grasp to comprehend the construction of artificial networks. Neurons are the basic building blocks of the central nervous system. Dendrites, cell bodies, and axons are the three primary components of a neuron. The dendrites receive signals from nearby neurons. The cell's dendrites deliver messages to the cell's body. The neuron nucleus is found in the cell body. When the neuron targets by sending an electrical signal beside the axon to the next neuron, the sum of the received signals exceeds a threshold value. The artificial neuron model is based on the human neuron's components, as shown in Figures 7 and 8. Dendrites are represented by the inputs X_0-X_3. The weights W_0-W_3 are multiplied by each input. From Figure 7, it is observed that Y is the output and F is the total summation of the inputs modelled neurons.

3.2. Design of Adaptive NFC. For designing NFC, we spot the controller from two spots explained in the following: in the first approach, the controller is depicted as a set of rules, which accepts the input in the form of qualitative variables and gives the output in the form of linguistic qualitative. The main advantages of such a system are as follows. Approximate knowledge about the plant is required, and an exact system model is not required. Knowledge representation and inference are easy. Implementation is easy. The fuzzy controller is one rule-based control system. One of the important advantages of using a fuzzy viewpoint is that the FL provides the best methods for knowledge depiction that could be devised for encoding knowledge about continuous variables. Figure 7 represents the model of a fuzzy system, which is composed of four major parts.

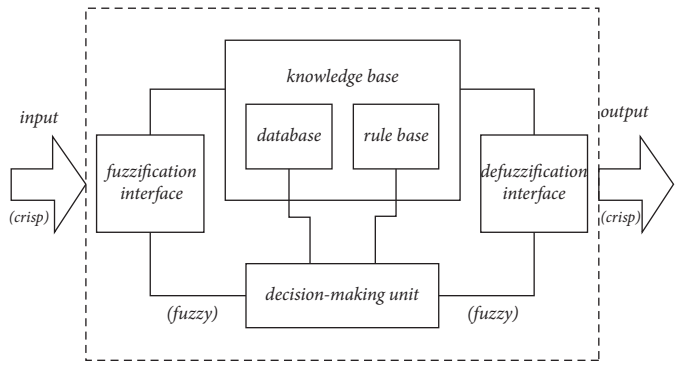

Figure 6: The general model of a fuzzy system.

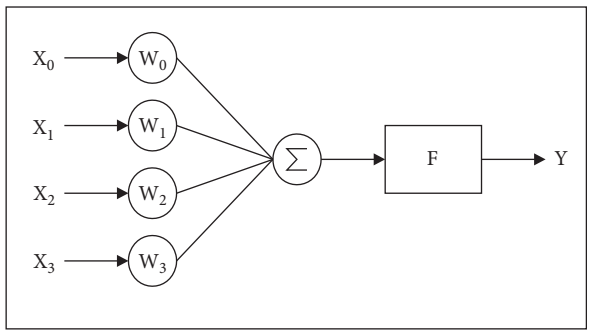

Figure 7: Neuro-fuzzy network structure [13].

Figure 5 shows the membership function of error and derivative of error between the output and reference of the controller used in this paper. "a" for this application is 0.5. The fuzzy inference table is shown in Figure 4. The second approach depicts the controller as a nonlinear map among the inputs and outputs. Depending on a specific plant, the map (in the form of a network) can be trained to implement any control plan. NNs, with their massive parallelism and ability to learn any nonlinearity, are used to address some of the practical control problems. An NN-based control system performs a particular form of adaptive control, with the controller taking the form of a multilayer network. The adjustable parameters are defined as the adaptable weights.

4. Learning in Adaptive NFC

The controller has to design as per the human's mimic actions in a few specific conditions. This design is based on the learning algorithm called the supervised learning algorithm for a system to be controlled. An artificial neural network is the best controller to control the system with the help of a supervised learning algorithm. The suitable learning algorithm will be used from the neural networks forward model. Nevertheless, in this case, the network input information is obtained from the human through the senor working principle. Then the output will be controlled by the human's input. The artificial-based supervisory learning algorithm that has been developed for the BLDC motor is shown in Figure 9. Figure 10 clarifies the block diagram of the supervisory algorithm of artificial neural networks to the BLDC motor. The error backpropagation (EBP) algorithm is a simple and easily understandable algorithm for neural network training [15]. Therefore, the controller will accept the output error in the system by using the EBP algorithm. Nevertheless, this method suffers from noise sensitivity and harmonics distortion, which will have a minimum effect on the system [12].

At least one supervisor should be connected to the EBP algorithm to improve the learning algorithm capacity and repeat its accurate, high-performance operation near the exact value. System performance may improve in this process, and the network weights are updated based on the input value. Figure 11 gives information about the supervised algorithm using the NFC controller, which will find the error between the supervisor input and plant output designed and developed in MATLAB/Simulink [12].

The development of the control strategy for speed control of the BLDC motor with the proposed ANFIS controller is presented in Figure 2. It consists of two loops: an inner loop and an outer loop. The inner loop synchronizes the inverting gate signal with the motor's back electromotive force or rotor position. The outer loop controls the speed of the BLDC motor by controlling the DC bus voltage through the PWM inverter. Based on the error and the rate of change of error, the BLDC motor drive system is designed and developed in the MATLAB; as shown in Figure 12, and the ANFIS controller provides the control signal to the switching logic circuit. The switching logic circuit provides the PWM signal for the inverter gate concerning the rotor position of the motor and the control signal output obtained from the ANFIS controller [18].

When the converter circuit is connected among the motor drive and load, the capacitor DC-link gets discharged within a short period. The execution of neuro-fuzzy controllers with the adapted torque control is shown in Figure 13. As a result, the currents are in peak value, which causes accruing spikes from the supply to the load side. These spikes will weaken the performance of the power factor and the overall system performance. However, the converters will maintain a good power factor using the VSI-designed converters. Figure 14(a) shows the phase voltage waveforms based on the rotor position at 900 rpm. The phase difference between a, V_b, and V_c is approximately 120°, and

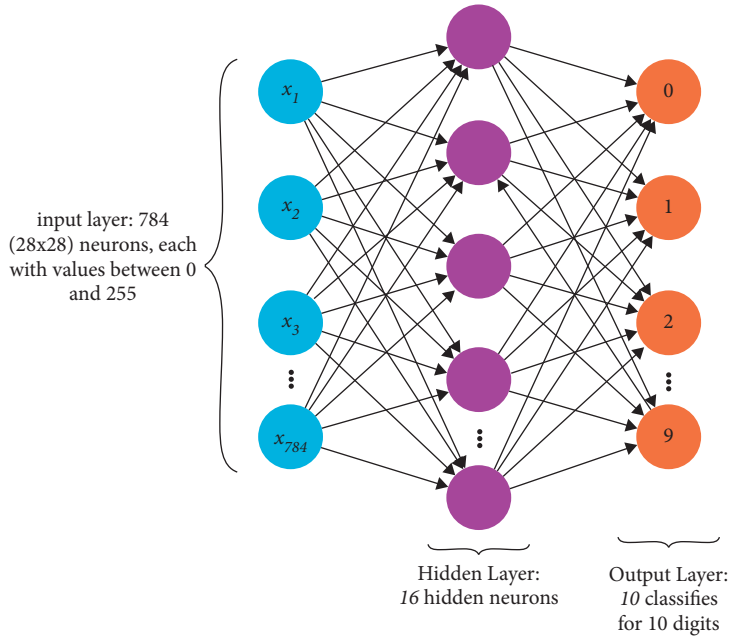

Figure 8: Multilayered artificial neural networks [13].

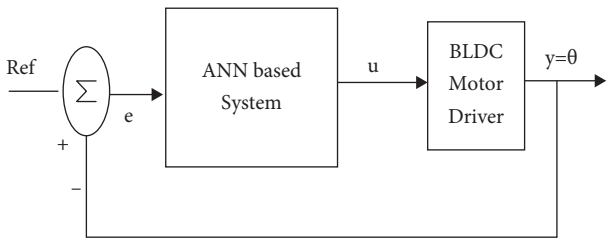

Figure 9: Supervisory control algorithm for the system.

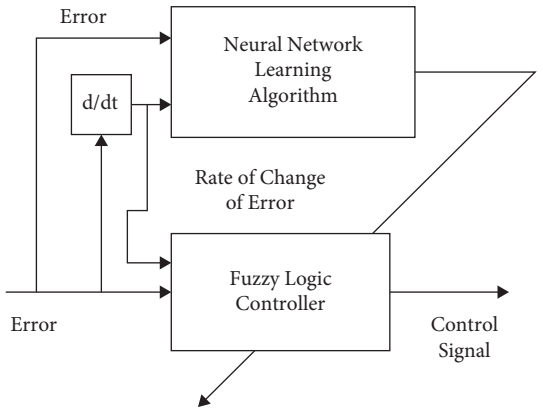

Figure 10: Block diagram of the supervisory controller of the system.

this result is designed with the artificial neural networks, and is also compared with Figure 14(b) which is designed with ANFIS controllers. The DC voltage of the BLDC motor is same in both cases of ANN and ANFIS, but the difference is in the power factor where it is lagging in ANFIS compared to ANN.

Furthermore, the above figure shows that the system has better source efficiency and minimized peak current levels, which causes the overall approach's cost to be minimized [16]. As the results show, the electromagnetic field of the BLDC motor for each phase is shown in Figure 15. It is observed the electromagnetic field is almost stable after 5 sec. The rotor of the BLDC motor and the permanent-magnet rotor follow the stator rotating magnetic field up to its equality, as shown in Figure 16. When the EMF is equal between rotor EMF and stator EMF, the motor produces the negligible harmonics shown in Figure 17.

As most applications demand, the drive must perform under varying load conditions. Therefore, to ascertain the superior performance of the proposed ANFIS controller, simulation results have also been obtained for varying load conditions. When the BLDC motor is running with load, the torque characteristics are shown in Figure 18. From Table 1 the minimum of load torque will be considered 0.7 Nm for the motor which is running at 700–900 rpm shown in Table 2, and it is observed that the reference torques and BLDC motor torque is uniform upper and lower limits from 1.3 Nm to 3.2 Nm. First, the load torque decreases from 3.2 Nm to 1.3 Nm and increases from 3.2 Nm to 3.5 Nm. The BLDC motor drive suffers from electromagnetic torque distortions due to the armature currents. The armature currents are generated during the armature windings' six-step switching conditions, which produces the harmonics. Here the electromagnetic toque decreases the harmonics with the proposed controllers by 1.0 to 1.3% using the mutual compensation of the magnetic winding sets within the switching angle of 60° electrical. In the air gap of

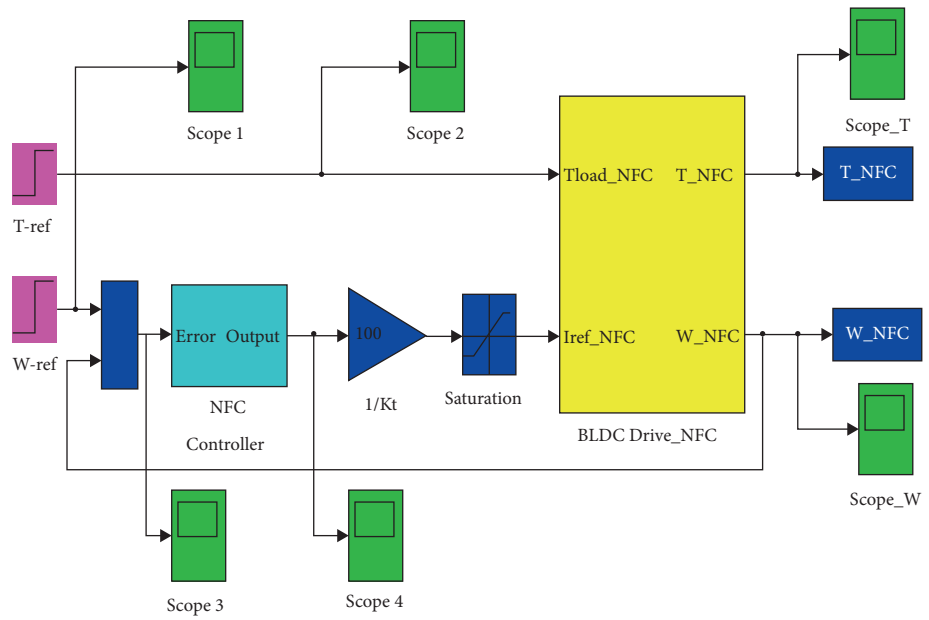

Figure 11: Block diagram of the system in Simulink [17].

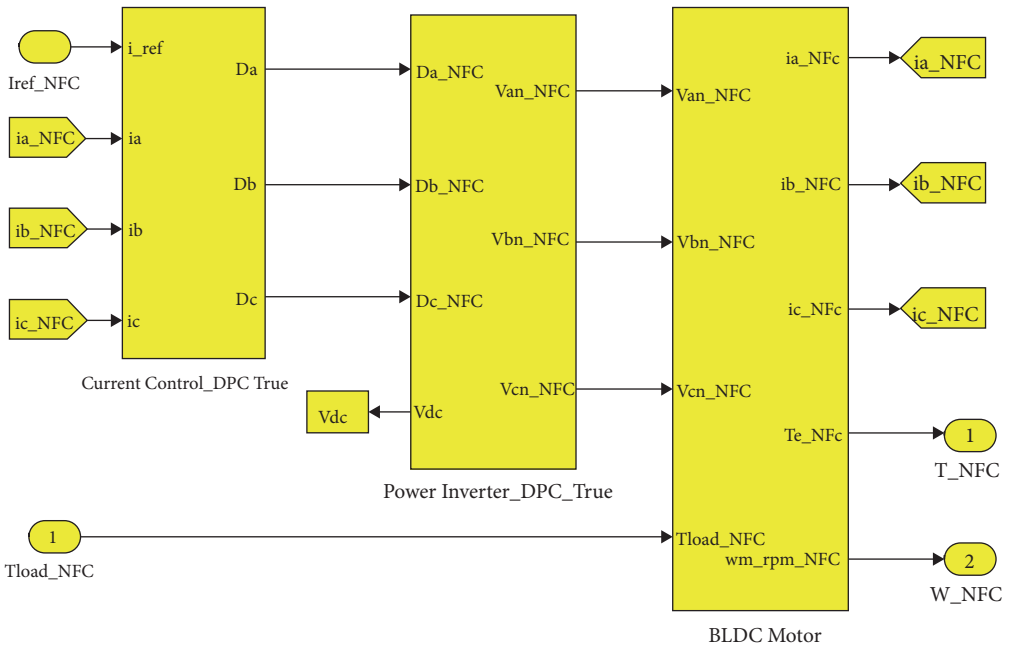

Figure 12: BLDC motor drive in Simulink [17].

the BLDC motor, the stator of will produces the stationary magnetic flux in the motor air gap. Figures 17(a) and 17(b) give information about the rotation of the rotor in this field that induces ac currents in its windings. The frequency of these currents decreases with rotor speed to set up a stationary magnetic field concerning the stator. The interaction of the two fields creates a braking torque whose magnitude depends on the dc field generated by the stator, the rotor resistance, and the speed of the rotor.

Figure 19 shows the active power and speed of the BLDC motor. Furthermore, the reference and BLDC motor speeds are compared with their desired values and implemented with the artificial neural networks. Finally, the torque of the BLDC motor is reached with its reference toque in Figure 19(c).

Figure 20 clarifies the improvement of the BLDC motor speed and torque, which is designed with the ANFIS controllers compared to the ANN controller. In optimizing the

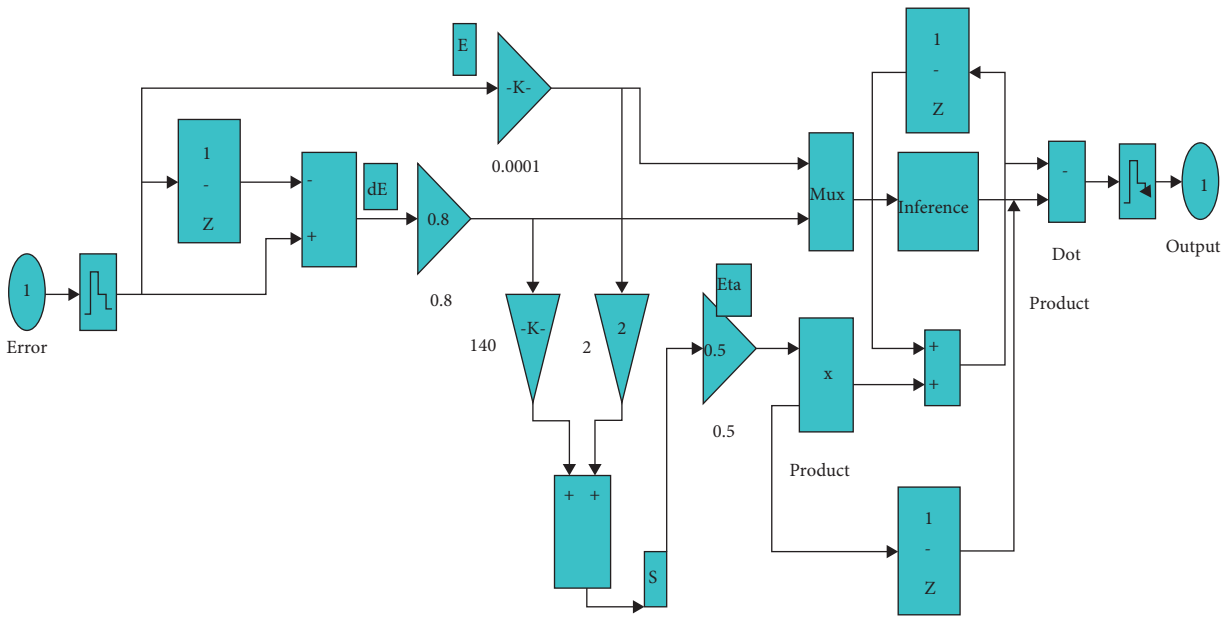

Figure 13: Execution of neuro-fuzzy controllers with the adapted torque control [17].

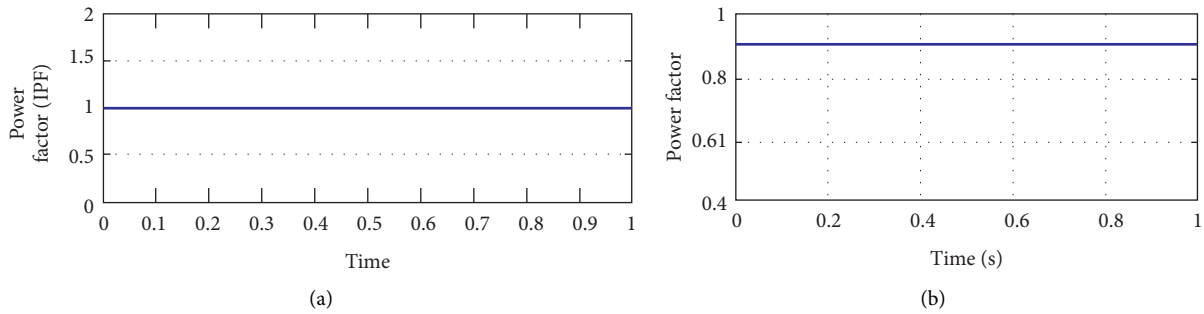

Figure 14: (a) ANN designed power factor. (b) ANFIS designed power factor.

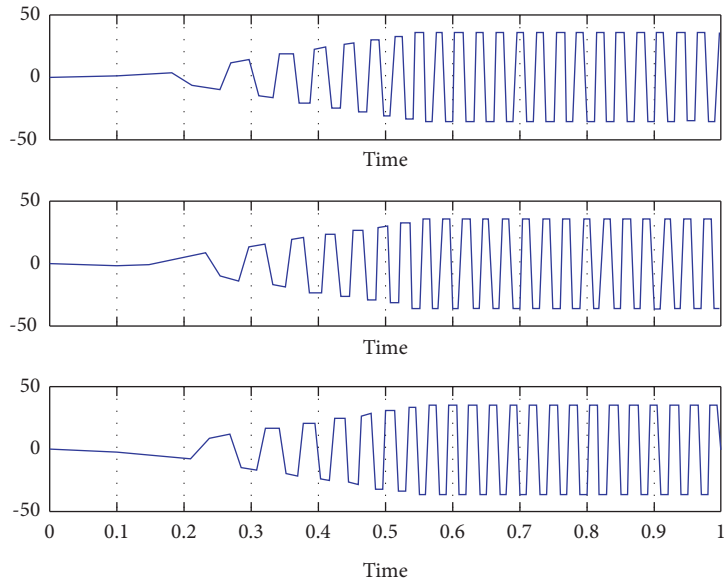

Figure 15: Stator back EMF e_a, e_b, and e_c of the BLDC motor.

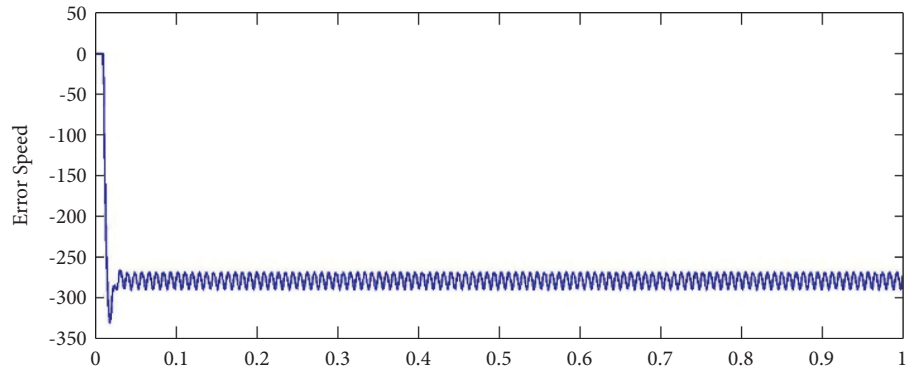

Figure 16: Rotor speed of BLDC motor.

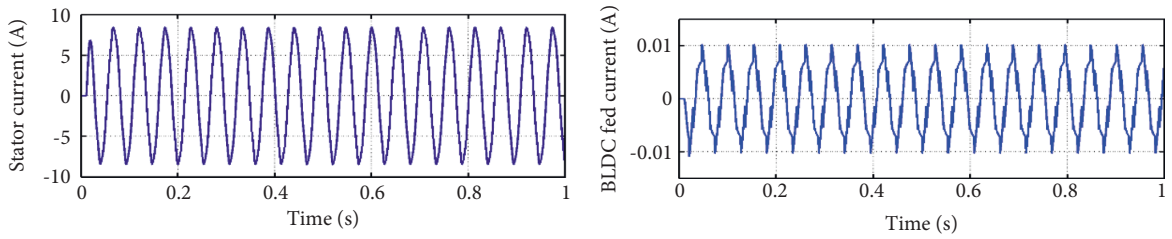

(a) (b)

Figure 17: (a, b) Stator currents of BLDC motor.

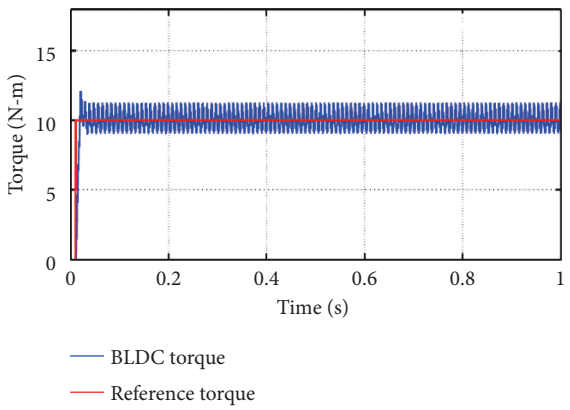

Figure 18: Electromagnetic torque T_E of the BLDC motor.

Table 1: Parameters of the BLDCM.

Parameter	Value
VDC	210 V
Flux linkages constant	0.107 [wb]
Self-inductance	2.72 mH
Mutual inductance	1.5 mH
Moment of inertia	0.000310 kg-m/sec^2
Resistance/Ph	0.72 [Ohm]
HP	3
K_t	0.21 [N.m/A]
Rated speed	3000 [rpm]
Rated power	1000 [Watts]
T_L	0.7 [N.m]

Table 2: Parameters of the BLDCM.

Parameters		ANN
Rise time	0–700 RPM	0.003
	700–900 RPM	0.003
Settling time	0–700 RPM	0.020
	700–900 RPM	0.003
Steady-state error	0–700 RPM	0.7%
	700–900 RPM	0.9%
Startup torque	0–700 RPM	3.2 N.N
	700–900 RPM	1.3 N.M
Startup current	0–700 RPM	3A
	700–900 RPM	1A
Speed variation	0.7%	0.6%
Power factor	0.7	0.8

current distortion and torque reduction in the BLDC motor, a suitable ANFIS controller is designed and implemented as a universal optimizer to find the optimized harmonics. Therefore, this proposed concept is designed and developed in three stages to minimize the distortion, where AI controllers have implemented optimized TPBLDCM. It is also considered to evaluate and improve the effectiveness and performance issues of the BLDC motor with this proposed algorithm. Finally, this concept will be implemented in Simulink/MATLAB with a comparative analysis of the BLDC motor and its modelling. The results encourage better performance than the conventional controllers. Figure 17 shows the simulation result of the phase current waveforms based on the rotor position at 700–900 rpm which is shown in Table 2. The peak current value is about 3 A for all I_a, I_b,

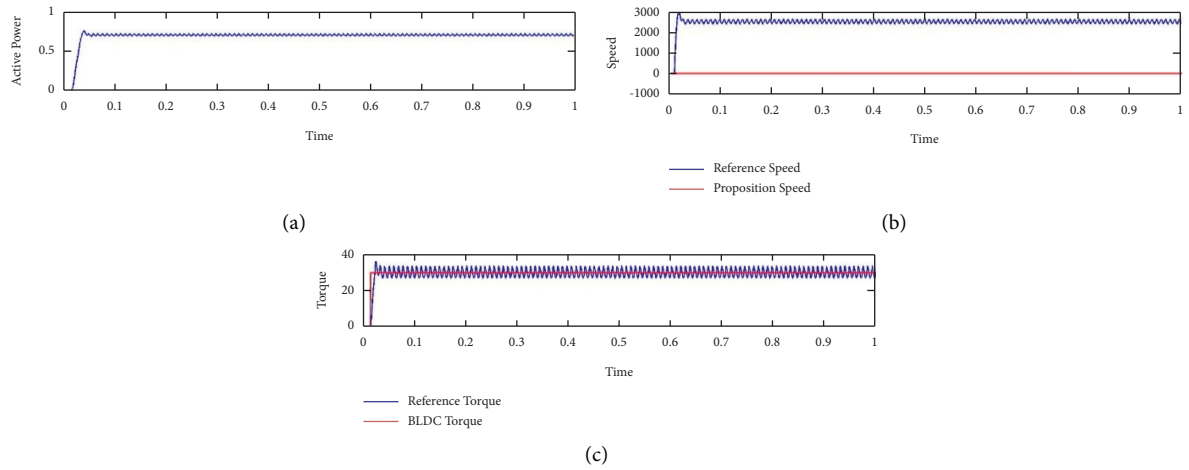

Figure 19: ANN designed. (a) Active power. (b) Reference speed and propulsion speed. (c) Reference torque and BLDCM torque of the BLDC motor.

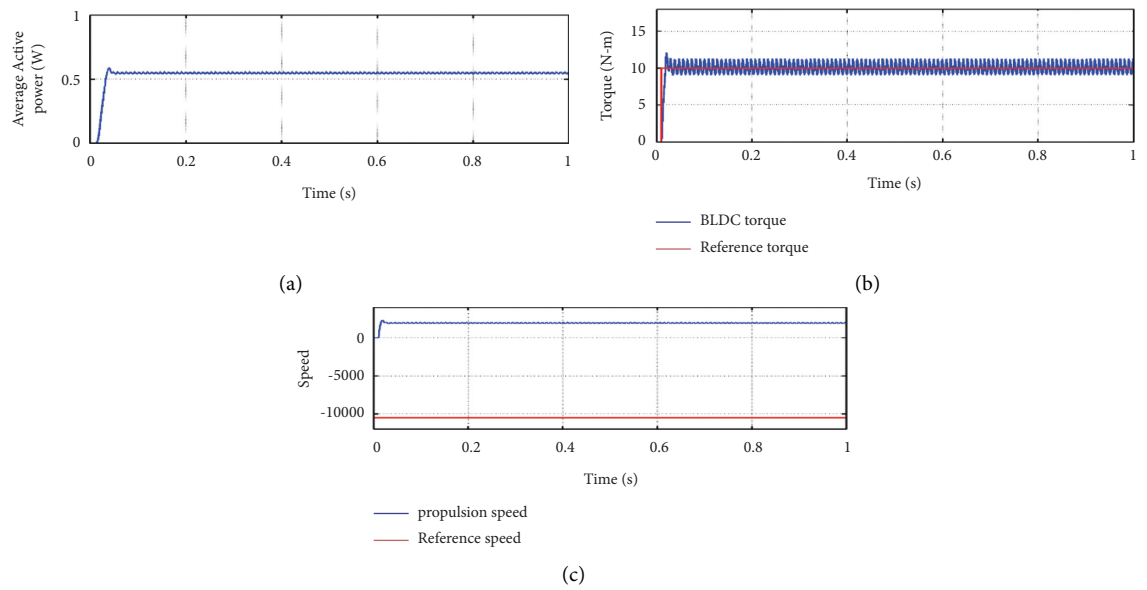

Figure 20: ANFIS designed. (a) Active power. (b) Reference speed and propulsion speed. (c) Reference torque and BLDCM torque.

and I_c, and steady state current varies from 0.7% to 0.9% with respect to the rise time shown in Table 2.

5. Conclusion

This paper concludes that the design of the neuro-fuzzy controllers is an effective controller for optimizing the disturbances and increasing the speed of the motor drive. The proposed controllers are the ANFIS controllers which will be designed with the suitable supervisory learning algorithm. Fuzzy logic control is designed with the 25 membership functions and connected to the four layers of artificial neural networks with two inputs and the derivative error. The gradient descent method of the supervisory learning algorithm for the ANFIS improves its operation because of its simple designed structure, learning capability, and high robustness against distortions, high-speed torque disturbances, uncertain hidden layers, and precise accuracy. This controller will act as an independent controller to the entire system's plant and will be applied to any nonlinear and uncertain approach. These ANFIS controllers also perform better than the PID controllers in tracking the reference speed, lower overshoot, optimized settling time, and low ripples with high-tracking efficiency.

Data Availability

The data are available upon request.

Conflicts of Interest

The authors declare that they have no conflicts of interest.

References

[1] S. Sivakotiah and J. Rekha, "Speed control of brushless DC motor on resonant pole inverter using a fuzzy logic controller," *International Journal of Engineering Science and Technology*, vol. 3, no. 10, pp. 7360–7357, 2011.

[2] S. A. Niapour, G. H. Garjan, M. Shafiei, M. R. Feyzi, S. Danyali, and M. Bahrami Kouhshahi, "Review of permanent-magnet brushless DC motor basic drives based on analysis and simulation study," *International Review of Economics Education*, vol. 9, no. 5, pp. 930–957, 2014.

[3] M. H. Rashid, "Power electronics: circuits, devices, and applications," *Pearson Education India*, vol. 76, pp. 778–789, 2009.

[4] A. Rubaai, R. Ricketts, and M. Kankam, "Development and implementation of an adaptive fuzzy-neural-network controller for brushless drives," *IEEE Transactions on Industry Applications*, vol. 38, no. 2, pp. 441–447, 2002.

[5] K. Sujatha, K. Naga, V. Vaisakh, and G. Anand, "Artificial intelligence-based speed control of brushless DC motor," *IEEE PES General Meeting. IEEE*, vol. 776, 2010.

[6] F. Mosavi and R. Mohammad, "Design of efficient adaptive neuro-fuzzy controller based on supervisory learning capable for speed and torque control of BLDC motor," *Przeglad Elektrotechniczny*, vol. 88, pp. 238–246, 2012.

[7] J. S. R. Jang, "ANFIS: adaptive-network-based fuzzy inference system," in *Proceedings of the IEEE Transactions on Systems, Man, and Cybernetics*, vol. 23, no. 3, pp. 665–685, June 1993.

[8] A. H. Niasar, H. Moghbelli, and A. Vahedi, "Modeling, simulation and implementation of four-switch, Brushless DC motor drive based on switching functions," *IEEE EUROCON 2009*, vol. 667, 2009.

[9] A. Abraham, "Neuro-fuzzy systems: state-of-the-art modelling techniques," in *Proceedings of the International Work-Conference on Artificial Neural Networks*, p. 444, Springer, Berlin, Heidelberg, June 2021.

[10] G. MadhusudhanaRao, Ch. Vinay Kumar, and A. RaghuRam, "Fuzzy based vector control method for BLDC motor drive with five-switch three-phase topology," *PalArch's Journal of Archaeology of Egypt/Egyptology*, vol. 17, no. 12, pp. 147–160, 2020.

[11] N. A. Halvai, M. A. S. Masoum, and H. Moghbeli, "Adaptive neuro-fuzzy intelligent controller via emotional learning for indirect vector control (IVC) of induction motor drives," in *Proceedings of the 12th Iranian Conference on Electrical Engineering*, p. 226, IEEE, May 2004.

[12] J. Žilkova, J. Timko, and P. Girovský, "Nonlinear system control using neural networks," *Acta Polytechnica Hungarica*, vol. 3, no. 4, pp. 85–94, 2006.

[13] Ch. Vinay Kumar, G. MadhusudhanaRao, and A. Raghu Ram, "AI based vector control method for BLDC motor with multi switch three-phase topology," *PSYCHOLOGY AND EDUCATION*, vol. 58, no. 1, pp. 3132–3141, 2021.

[14] B. Allaoua, A. Abdessalam, G. Brahim, and N. Abdelfatah, "Efficiency of particle swarm optimization applied on fuzzy logic DC motor speed control," *Serbian Journal of Electrical Engineering*, vol. 5, no. 2, pp. 247–262, 2008.

[15] C.-T. Lin and Y. C. Lu, "A neural fuzzy system with fuzzy supervised learning," *IEEE Transactions on Systems, Man, and Cybernetics-Part B: Cybernetics: A Publication of the IEEE Systems, Man, and Cybernetics Society*, vol. 26, no. 5, pp. 744–763, 1996.

[16] S. Singh and B. Singh, "Power factor correction in permanent magnet brushless DC motor drive using single-phase Cuk converter," *Journal of Engineering Science & Technology*, vol. 5, no. 4, pp. 412–425, 2010.

[17] J. Cao, "Torque ripple control of position-sensorless brushless DC motor based on neural network identification," in *Proceedings of the 2008 3rd IEEE Conference on Industrial Electronics and Applications*, IEEE, June 2008.

[18] K. Premkumar and B. V. Manikandan, "Adaptive neuro-fuzzy inference system based speed controller for brushless DC motor," *Neurocomputing*, vol. 138, pp. 260–270, 2014.